JOURNAL OF MATERIALS SCIENCE **34** (1999) 2535–2546

Fatigue damage mechanisms in unidirectional carbon-fibre-reinforced plastics

E. K. GAMSTEDT*
Department of Materials and Production Engineering, Luleå University of Technology, SE-97187 Luleå, Sweden

R. TALREJA
School of Aerospace Engineering, Georgia Institute of Technology, Atlanta, Georgia 30332-0150, USA

The fatigue life behaviour and the underlying micromechanisms have been studied in two different types of unidirectional carbon-fibre-reinforced plastics loaded in tension-tension along the fibre direction. The carbon fibres (AS4) were the same in the two composite systems. One thermoplastic matrix (polyetheretherketone, PEEK) and one thermosetting matrix (epoxy toughened with a thermoplastic additive) were used. The macroscopic fatigue behaviour was characterised by fatigue life diagrams. Surface replicas were taken intermittently during the course of the fatigue tests to monitor the active fatigue damage micromechanisms. The thermoset based composite showed a higher fatigue resistance with few microcracks initiated at distributed fibre breaks growing at a decelerating rate. The thermoplastic composite had a more pronounced fatigue degradation with a steeper fatigue life curve, which was caused by widespread propagating debonds and matrix cracks. The use of a tougher and more ductile matrix results in an inferior fatigue life performance, due to a more widely distributed accumulation of damage that propagates at a higher rate.

1. Introduction

1.1. Fatigue in CFRPs

Carbon-fibre-reinforced plastics (CFRPs) are widely used for load carrying structures where the specific strength and specific modulus are of importance, e.g. aircraft wings, helicopter rotor blades, and other aerospace applications. These structures are often subject to vibrations and other fluctuating loads, which cause fatigue degradation of the material. Fatigue is known to be responsible for the majority of failures of structural components [1]. For homogeneous materials like metals and alloys, fatigue design methodologies are generally based on the self-similar growth of a single dominant crack which eventually causes ultimate failure. The fatigue mechanisms in composite materials are more complex, and involve a multitude of spatially distributed and interacting mechanisms. Due to limited knowledge of the underlying mechanisms, design against fatigue in composites has been relied on empiricism based on extensive and costly testing.

The configuration of a composite laminate, i.e., its fibre orientations and stacking sequence, must be chosen to meet the design needs. Presently, each new configuration is regarded as a new material and its fatigue behaviour is determined experimentally. This situation will improve if the effects of constituent properties and fibre architecture on the fatigue behaviour are understood. Talreja's fatigue life diagram [2], described below, provides a means of clarifying these effects qualitatively [3]. In one class of symmetric laminates that have longitudinal unidirectional plies and are loaded in cyclic tension along these plies, the laminate fatigue is found to be governed by the fatigue of these plies [3–5]. For this reason, understanding the fatigue behaviour of unidirectional composites is of paramount importance. This paper is aimed at achieving this with the specific objective of clarifying the role of the polymeric matrix. Two unidirectional composites with the same carbon fibres and different matrix materials, a rubber modified epoxy and a thermoplastic, are studied. The micromechanisms governing in the different regimes of the fatigue life diagram are described. Finally, implications of the obtained results on models aimed at fatigue life prediction are discussed.

1.2. Fatigue life diagrams

Conventionally, fatigue data are plotted in one or the other form of a Wöhler diagram where a stress value (amplitude, maximum, etc.) is plotted against logarithm of the number of cycles to failure. Talreja [2] argued that for composite materials this type of diagram did not adequately represent the multitude of underlying damage

* Present address: Materials Research Department, Risø National Laboratory, P.O. Box 49, DK-4000 Roskilde, Denmark. E-mail: kristofer.gamstedt@risoe.dk.

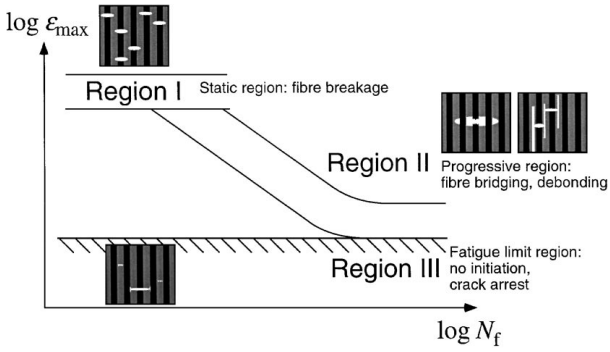

Figure 1 Fatigue life diagram of longitudinal composites in tension-tension fatigue.

mechanisms. He instead proposed a framework, called fatigue life diagram, to facilitate interpretation of the fatigue mechanisms and their relative roles. The diagram plots the peak strain achieved in the first load cycle in a constant-amplitude load-controlled test against logarithm of the number of cycles to failure. Three regions are then argued to exist in the diagram on the basis of the nature and characteristics of the underlying damage mechanisms. For unidirectional composites loaded in cyclic tension along fibres, the fatigue life diagram is illustrated schematically in Fig. 1. Region I in the diagram is a horizontal scatter band placed to coincide with the static failure scatter range at the first half-cycle of load. The horizontal orientation of this region reprsents the non-progressive nature of the underlying mechanism of fibre failure. At a certain range of cycles, dependent on the constituent properties, Region II, indicated by a sloping band of scatter on the fatigue life, begins. The progressive mechanisms of fatigue failure in this region are fibre-bridged matrix cracking and fibre/matrix debonding. This region asymptotically approaches a limiting value, below which Region III of no failure exists. The mechanisms in Region III are either arrested or have too low rates of progression to cause failure in a large number of cycles. A method based on statistical analysis of fatigue life data has been proposed [6] to partition data in the three regions and thereby make a systematic comparison of candidate material behaviour. Talreja [3] has presented a thorough discussion of the use of the fatigue life diagram in a consistent interpretation of the roles of matrix toughness and fibre architecture in composite fatigue.

1.3. Influence of matrix toughness

The polymer industry has over the years produced a large number of thermosetting resins and thermoplastics for use as matrix materials in composites. It is often implicitly assumed that improvements in ductility, toughness and fracture toughness of neat resins will lead to improvements in the same properties of composites as well. While the fibre architectural aspects in laminates are bound to affect such improvements, even for unidirectional composites it is not clear whether the improvements hold under long-term loading. It has been argued that for composites with fibres of high strain to failure (∼2%) higher ductility of resin will be beneficial and a comparison of composites with different failure strains of fibres and matrix indicated improvement in fatigue life due to higher matrix ductility [7]. Other researchers have been found that an increase in the static delamination fracture toughness under static conditions was not matched by a corresponding increase in fatigue resistance to delamination [8, 9]. Moreover, composites with tougher matrices are found to degrade faster in fatigue as indicated by the slope of the strain vs. life plot (Region II of fatigue life diagram) [10, 11]. For instance, at equal strain levels, unidirectional carbon fibres (CF) in polyetheretherketone (PEEK) show lower fatigue life than CF/epoxy [10]. In an effort to understand this anomalous behaviour, Curtis [12] found a more rapid growth of longitudinal splits from drilled holes in unidirectional CF/PEEK compared to CF/epoxy. The adverse effects of matrix toughness on fatigue behaviour in metal matrix composites have been discussed in [13].

2. Experimental

2.1. Materials and processing

Two CFRP materials were studied, CF/epoxy and CF/PEEK. The CF/epoxy was AS4/8552 from Hercules with a polyethersulfone (PES) modified matrix for increased toughness compared to standard brittle epoxy. The CF/PEEK was APC-2 from ICI Ltd. The two composite materials had the same AS4 carbon fibres, and were prepared by stacking four unidirectional plies.

The CF/epoxy was manufactured in an autoclave according to the manufacturers' recommendations at 120 °C and 6 bar for 2 hours. During the autoclave process, a well polished plate of stainless steel was placed inside the vacuum bag directly on top of the release film covering the stacked prepreg plies. This was to enhance the surface smoothness and to prevent the usual texture on the upper surface of the composite from the release fabric or surface bleeder. As a result, more excess resin was bled than for a conventional cure process without a pressure plate, and a fibre volume fraction of ∼63% was obtained.

The CF/PEEK prepregs were stacked and covered with smooth release coated aluminum foils, and heated between thick steel plates for 10 minutes at 400 °C. Thereafter, the laminate and plates were immediately brought to a hot press which held a temperature of 260 °C. The laminate was press moulded for 10 minutes, whereupon the heating system was turned off, and the composite was cooled down under pressure to avoid curvature. The thickness of the steel plates was 20 mm to assure a moderate cooling rate. The cooling rate is known to have a noticeable influence on the fatigue properties of CF/PEEK [14, 15]. Since the cooling rate was not accurately measured here, the degree of crystallinity of the matrix was instead determined by differential scanning calorimetry (DSC), and found to be 36%. The approximate volume fraction of fibres was determined from the etched cross-sectional surface by image analysis, and found to attain ∼60%.

The specimens were cut to dimensions according to ASTM standard D3039—a 127 mm gage length, 12.7 mm width, and 0.5 mm thickness. Tapered glass fabric/epoxy end tabs were bonded to the laminates with an adhesive epoxy film. In particular for the CF/PEEK

material, it was important to roughen the end tabs and the laminate surface with sand paper before gluing to avoid tab delamination during testing. The specimen edges were polished with a successively finer silicon carbide paper ending with 2400 grit. Before testing, the specimens were stored in a dessicator.

TABLE I Static longitudinal properties of the CFRPs

Property	CF/epoxy	CF/PEEK
Strength, σ_u	1.63 GPa	1.99 GPa
Strain to failure, ε_u	1.27%	1.50%
Young's modulus, E	129 GPa	133 GPa
Poisson's ratio, ν	0.29	0.28

2.2. Test methods

The mechanical tests were performed on an Instron 1272 tensile machine with hydraulic grips. The fatigue tests were load controlled with sinusoidal loading and a stress ratio of $R = 0.1$. The frequency of 10 Hz was selected as a compromise between autogeneous heating and reasonable test durations. On occasions during fatigue testing, a thermocouple was applied to the surface, and indicated an increase in temperature less than 2 °C. All tests were done at room temperature.

Cellulose acetate films were used for surface replication during the course of the fatigue testing. Before replication, the surface was carefully cleaned with alcohol and let to dry. The replicas were made malleable with an acetone based solution, and pressed onto a predesignated spot on the flat surface of the specimens for 2 minutes. The peak load was applied during replication to allow the cracks to open and become visible. The replicas were then let to harden. They were stored under a microscope glass, on which a heavy object was placed to prevent them from curling. A carbon layer was sputtered onto the replicas to improve the contrast of the micrographs. By finding large damage sites in the replica with the highest number of cycles, and relocating the same damage site in replicas with lower number of cycles, a sequence of micrographs with progressive fatigue damage could be put together. Since the damage sites often were dispersed and rare, a map with reference points such as scratches, misaligned fibres etc. had to be drawn in order to relocate the position of the fatigue damage. Moreover, repeated applications on dummy samples were done to confirm that the replica solvent did not degrade the composite surface. Optical microscopy was performed with a built-in microscope of a Matzusawa MXT-α microhardness tester connected to a computer for image analysis.

3. Results and discussion

3.1. Macroscopic fatigue behaviour

Mechanical properties of the two material systems from quasi-static tests are presented in Table I. Eight samples of each material were tested, and the scatter was less than 5% of the mean. It is noteworthy that the values of static properties of CF/PEEK are significantly higher than those of CF/epoxy. Since the strain to failure of the fibres are known to govern the strain to failure of unidirectional polymer matrix composites, the observed difference can be inferred from a batch to batch variability of the properties of the AS4 carbon fibres. The carbon fibres themselves are almost insensitive to fatigue [16]. This means that if the superior mechanical properties in CF/PEEK are not retained in fatigue, a deleterious progressive fatigue mechanisms related to the matrix or its interface to the fibres must must be active.

In Fig. 2, the fatigue life diagrams of CF/epoxy and CF/PEEK are plotted in terms of maximum initial strain vs. number of cycles to failure in logarithmic scales. The most striking features are that the CF/epoxy data have larger scatter, and that the CF/PEEK shows more fatigue degradation, i.e., the progressive Region II shows a steeper slope. Scatter in strength and lifetime is inherent in brittle materials. With brittleness is here

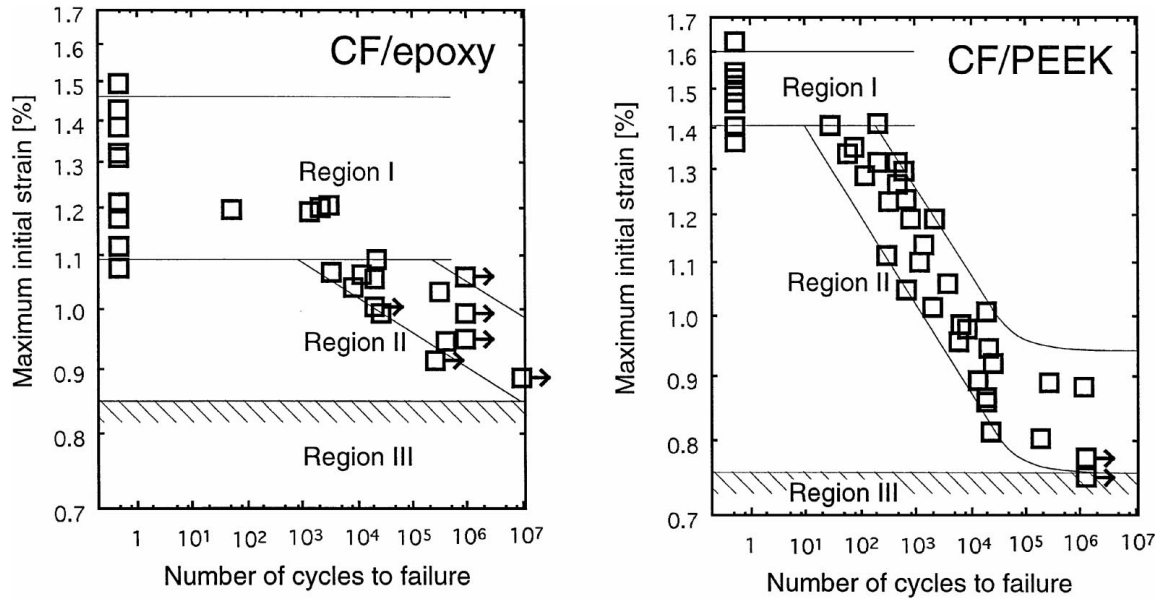

Figure 2 Fatigue life diagrams of CF/epoxy and CF/PEEK.

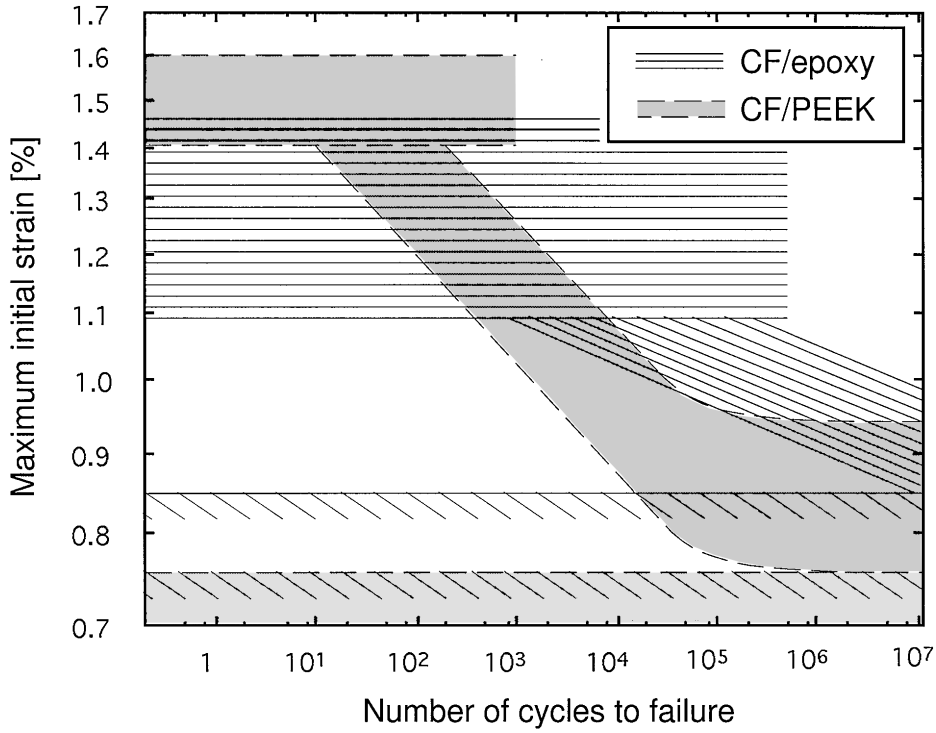

Figure 3 Comparison of fatigue life scatter bands of CF/epoxy and CF/PEEK.

meant that the ultimate strength is controlled by the largest flaw, and the inability to undergo inelastic deformation caused by accumulation of irreversible distributed damage. The sloping part in a fatigue life curve is indicative of progressive mechanism, i.e., sequential fibre breakage with a stress-dependent rate. The scatter bands of the fatigue life diagrams in Fig. 2 are superimposed for ease of comparison in Fig. 3. By comparing the fatigue behaviour of the two materials, it can be inferred that the use of the more ductile PEEK matrix results in some damage mechanism on the microscale which invokes a more rapid rupture process of fibres, and in turn a steeper slope in Region II. To investigate this proposition further, the active damage mechanisms were studied for the two materials.

3.2. Mechanisms in CF/epoxy

A sequence of micrographs taken in Region II of a propagating fibre-bridged crack in CF/epoxy is shown in Fig. 4. The crack tips took a deformed squeezed shape after a couple of hundred cycles of loading. The fibres have a distribution in strength, and some fibres will rupture at the first application of load, even though the strain is well below the static strain to failure of the unidirectional composite. From these fibre breaks, matrix cracks originated and grew transverse to the load and fibre direction. These cracks encountered neighbouring fibres, propagated past them and acquired a squeezed profile at the tips. Similar crack shapes have been observed in unidirectional metal-matrix composites due to bridging fibres [17, 18]. A schematic picture illustrating the principal appearance of a fibre-bridged crack which has been initiated from a single fibre break is presented in Fig. 5. In micrographs from some replicas, individual bridging fibres could be discerned (cf. Fig. 6). Since the bridging fibres exert a cohesive traction on the crack surfaces close to the crack tips, the stress intensity is subdued compared to an unbridged crack of the same size. Consequently, the propagation rate should be reduced by the bridging action.

The propagation rate of a uniform crack which grows in a self-similar manner is known to be described by

$$\frac{\mathrm{d}a}{\mathrm{d}N} = C(\Delta K)^m,$$

where a is the crack length, N is the number of cycles, ΔK is the range of the stress-intensity factor, and C and m are parameters that characterise the propagation rate. By integration of this relation, it can be shown that the crack growth accelerates with increasing number of cycles for non-critical fatigue at constant-amplitude loading. Contrary to this behaviour, the crack growth of the fibre-bridged cracks showed a decelerating trend (see Fig. 7). A contribution to the discrepancy between the anticipated accelerating growth and the observed decelerating growth is the bridging action itself. The bridging fibres effectively shields the crack tip by the cohesive traction (see e.g. Cox and Lo [19]). No progressive fibre breakage was recorded during fatigue, which indicates that the bridging fibres remain unbroken until the point of catastrophic failure.

The observed fibre-bridged cracks in CF/epoxy in Region II were scarce and distributed. It was only in the extreme vicinity of one another, that cracks showed tendencies to coalesce (see Figs 8 and 9). Cracks that were found close to one another usually emanated from a common surface scratch which arose during manufacturing of the specimen. Since crack coalescence was

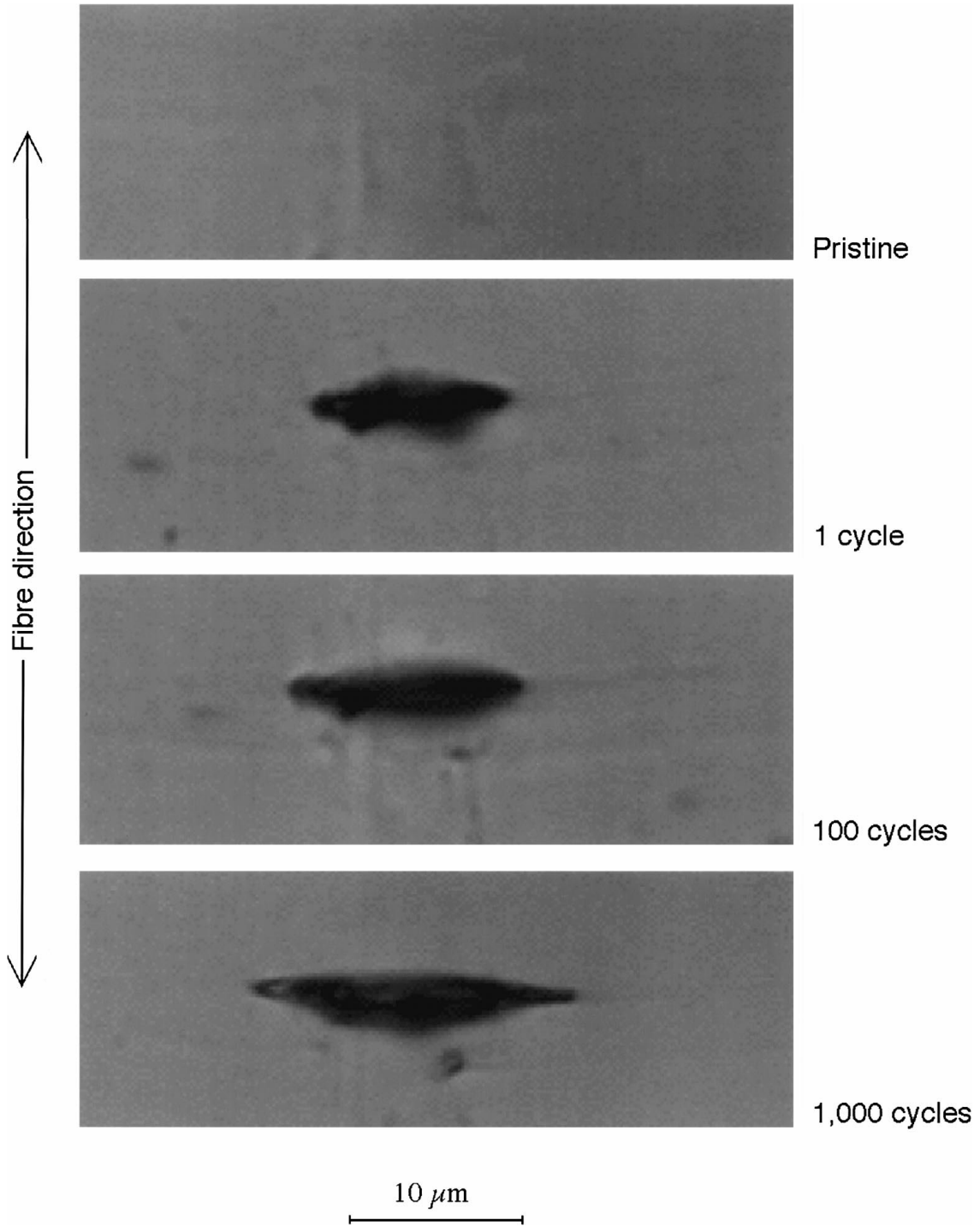

Figure 4 Fibre-bridged crack propagation in Region II in CF/epoxy (strain amplitude: $\varepsilon = 1.08\%$).

very uncommon, the cracks could generally be regarded as independent damage entities prior to catastrophic failure, which would facilitate the conception of a quantitative model of crack propagation.

In Region III, below the fatigue limit, there was a transition in mechanisms. Progressive growth of transverse fibre-bridged cracks was suppressed, and limited debonding along the fibre-matrix interface set in. In Fig. 10, a crack encompassing about 4 fibres at the surface is found. Debonding commenced after a few million of cycles at both crack tips. The debonds progressed at different rates and had a jagged and irregular appearance, which indicate an erratic and stochastic growth rate.

A typical type of damage found in Region III was a single fibre break from which debonds grew. An example of this damage type is shown in Fig. 11. The debond length can readily be measured, and plotted with respect to the number of cycles. Such a plot is found in Fig. 12. The four curves refer to one debond measurement each, i.e., the distance from the fibre-break plane to the debond crack tip on each side of the broken fibre. Notable is that the mode II debond growth retarded and became arrested after a few million cycles of loading. This was the case for all debonds observed in Region III. If the debonding were to persist and keep on growing, it is plausible that it would lead to successive breakage of nearby fibres and eventual failure. As a debond grows

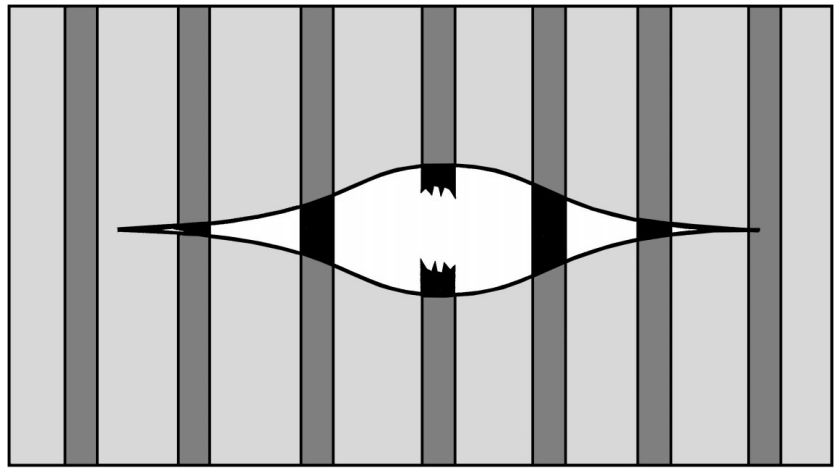

Figure 5 Schematic picture of fibre-bridged crack originating from a single fibre break.

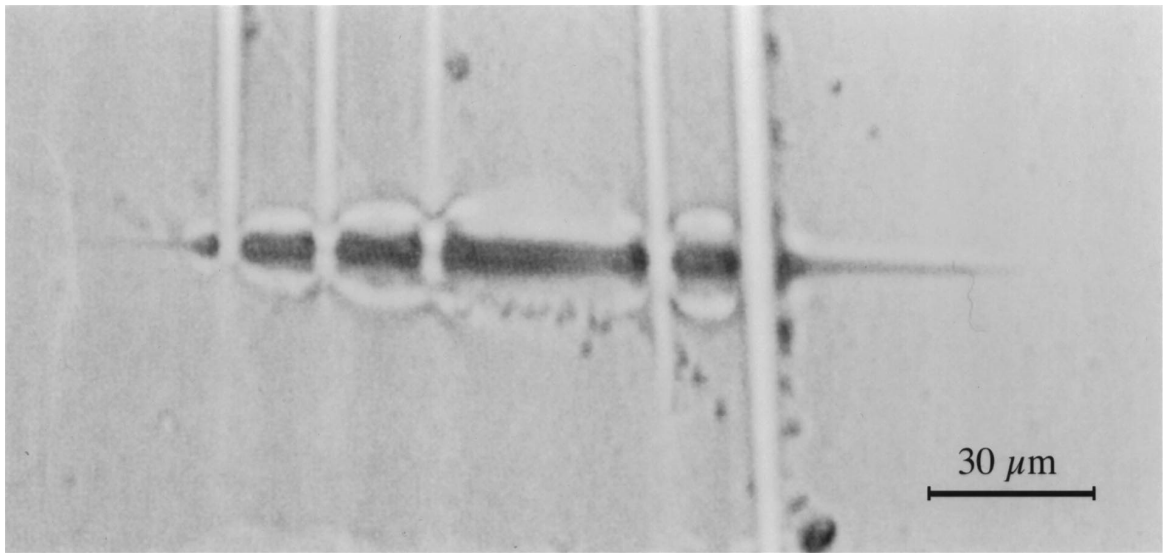

Figure 6 Crack with visible bridging fibres in Region II in CF/epoxy at 1,000 cycles ($\varepsilon = 1.08\%$).

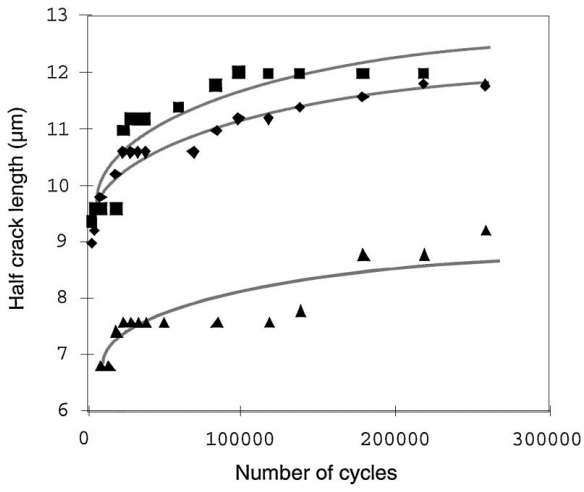

Figure 7 Propagation curves for bridged cracks in Region II in CF/epoxy ($\varepsilon = 0.92\%$).

extensively, the stress profile in the neighbouring fibres changes. Since the fibre strength has a distribution along the length of the fibre, non-aligned fibre breakage can be expected as a result of the propagating debond. In such a scenario, the debonding mechanism would act as a progressive mechanism, whereas in Region III in the CF/epoxy material, the limited debonding acted as a crack arresting mechanism.

The progressive fibre-bridged cracking mechanism was active in Region II, whereas the arresting debond mechanism prevailed in Region III. A transition in mechanisms from Region II to III as a matrix crack approaches a neighbouring fibre is schematically depicted in Fig. 13. The transition is controlled by the applied strain level, and the predominance of the two mechanisms precludes the presence of the other. Once debonding sets in, the progressive growth of fibre-bridged cracks, which ultimately leads to catastrophic failure, is suppressed. The driving force for further crack propagation is thus inhibited by the effective crack blunting. Observations of fatigue damage mechanisms in unidirectional metal-matrix composites indicate that the observed competing mechanisms are present in other material systems [20]. Since the transition in mechanisms occur at the fatigue limit, and this limit is frequently used in design, a thorough investigation of the governing microstructural properties should be undertaken.

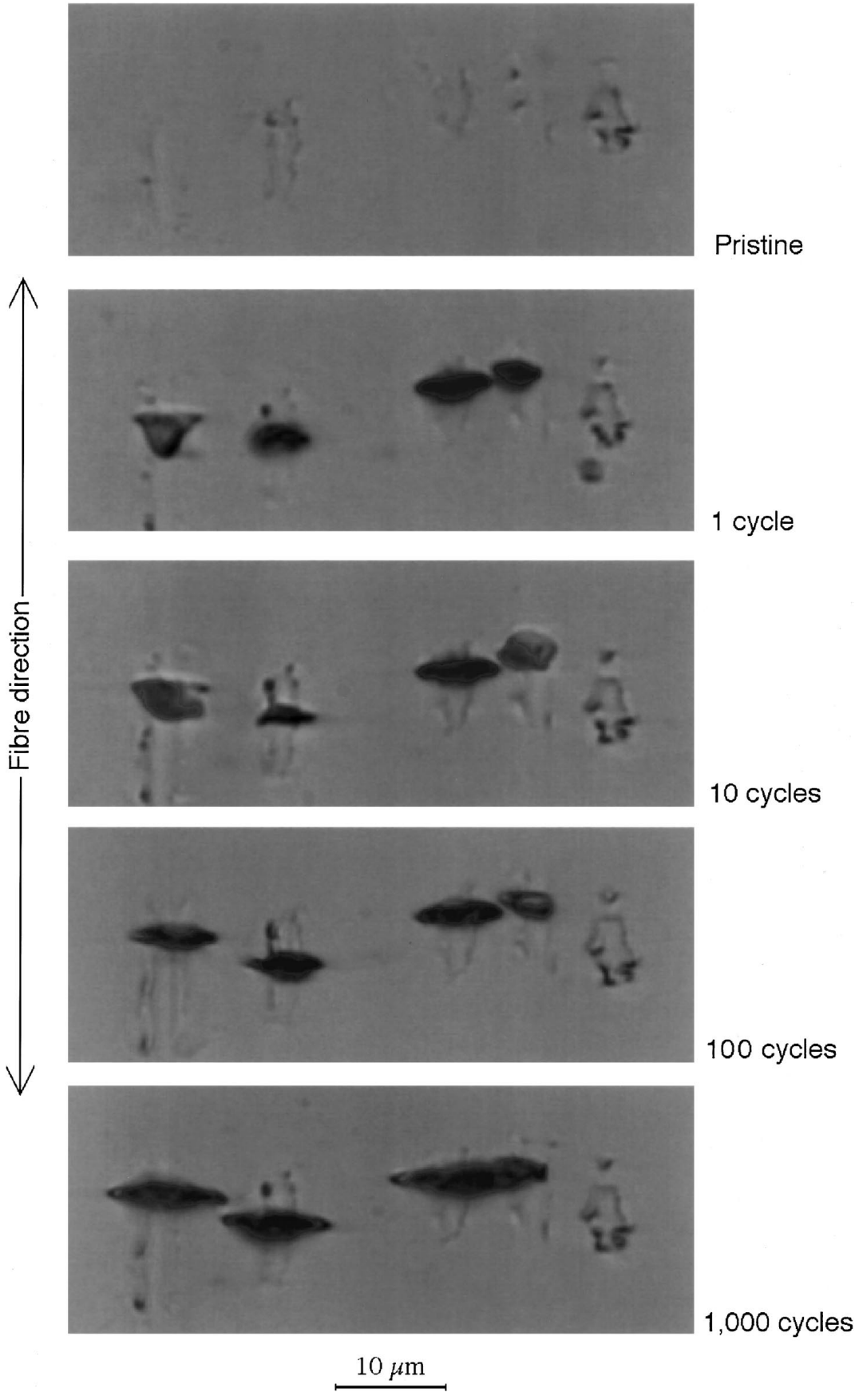

Figure 8 Propagation of neighbouring cracks in Region II in CF/epoxy ($\varepsilon = 1.08\%$).

3.3. Mechanisms in CF/PEEK

In the CF/PEEK material, the observed fatigue damage mechanisms were completely different from those observed in the CF/epoxy material. In Fig. 14, a series of replicas with fatigue-damage growth is shown. From the widespread pre-existing flaws, matrix cracks or debonds grew predominantly along the fibre direction. These cracks were abundant and ubiquitous at high

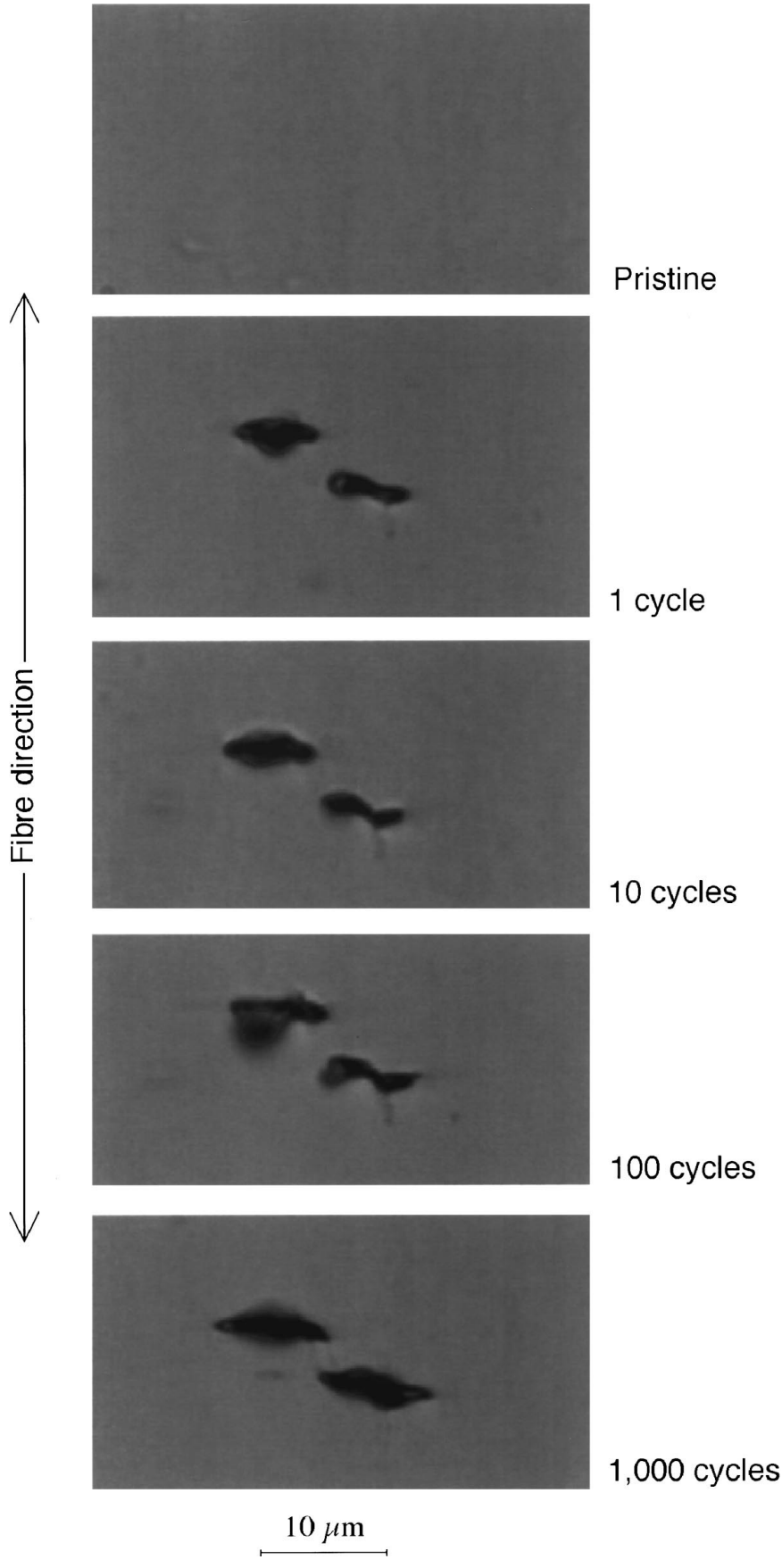

Figure 9 Tendency for crack coalescence in Region II in CF/epoxy ($\varepsilon = 1.08\%$).

cycles. The cracks grew in a random accelerating-decelerating manner, and became more pronounced during fatigue, which could be explained by the continuous cyclic wear at the crack surfaces. In contrast to CF/epoxy, successive breakage of fibres was detected during the course of the fatigue tests. A higher density of fibre breaks has also been observed in various polymer-matrix composites with toughened matrices

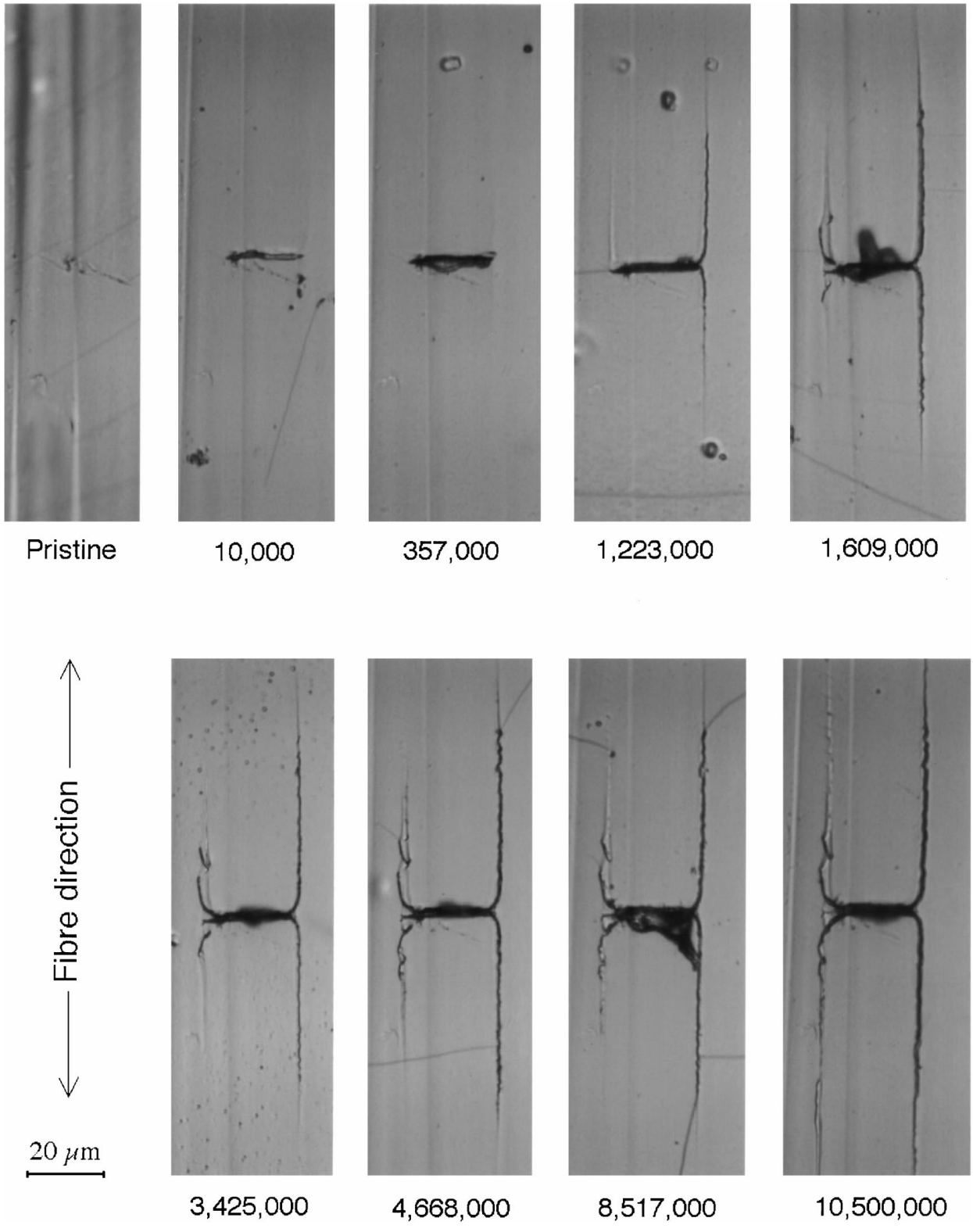

Figure 10 Debonding from a plane crack of fibre breaks in Region III in CF/epoxy ($\varepsilon = 0.89\%$).

compared composites with pristine matrices [21, 22]. The longitudinal cracks did not come to a halt and were substantially larger than the debonds observed in Region III in the CF/epoxy samples. Since these cracks kept on growing, which resulted in changing overloads in the neighbouring fibres, weak segments in these fibres would eventually fail. From the resulting fibre ruptures, new longitudinal cracking would emanate, etc. The sequential accumulation of fibre breaks and interaction with propagating longitudinal cracks lead to the observed widely distributed damage. No transition with competing mechanisms was observed at the fatigue limit. In Region III, the applied strain level was too low to provide a driving force for the progressive longitudinal cracking. The debonds and matrix cracks stopped growing at a short distance from their initiation locations, since the threshold for further propagation was not attained.

When debonds and localized matrix cracks link up, they will form large longitudinal splits. On a larger

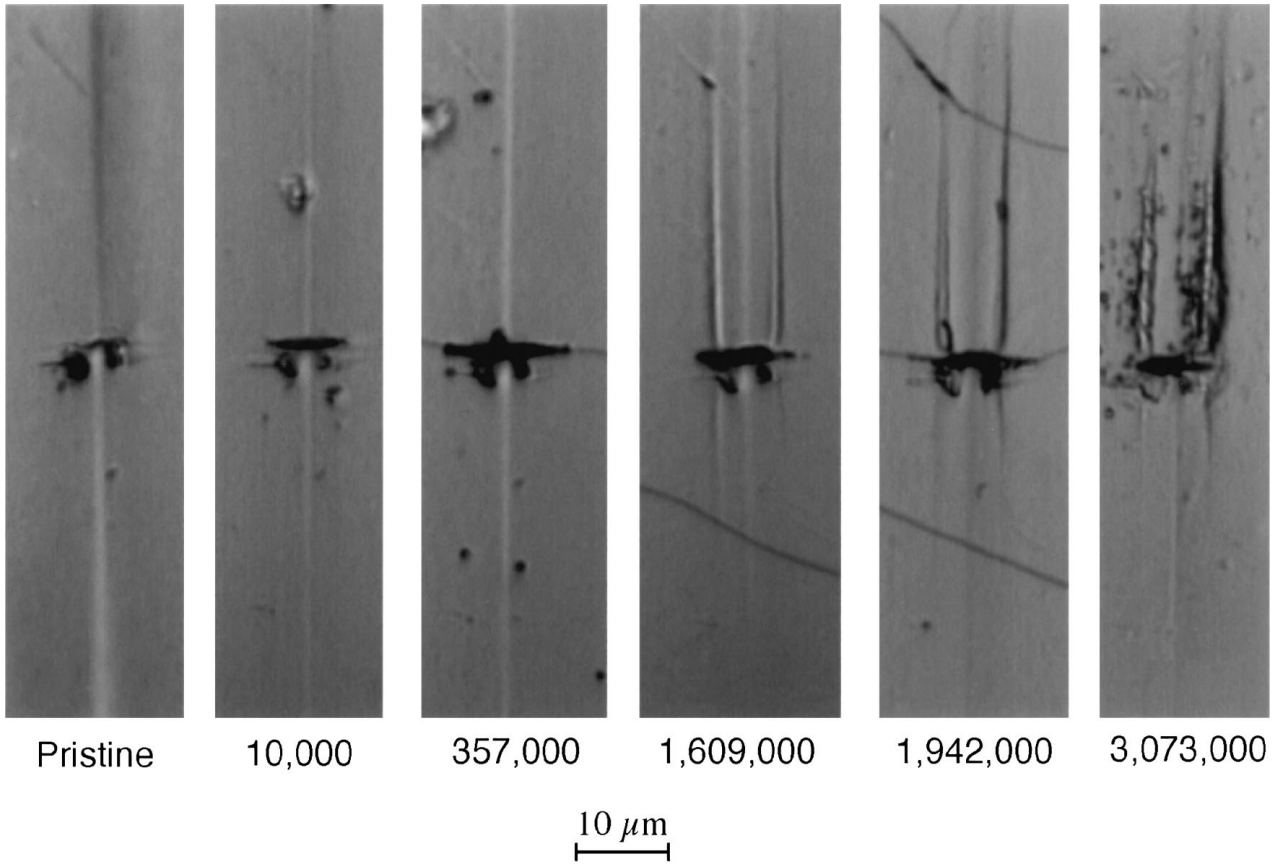

Figure 11 Debond growth from a single fibre break in Region III in CF/epoxy ($\varepsilon = 0.89\%$).

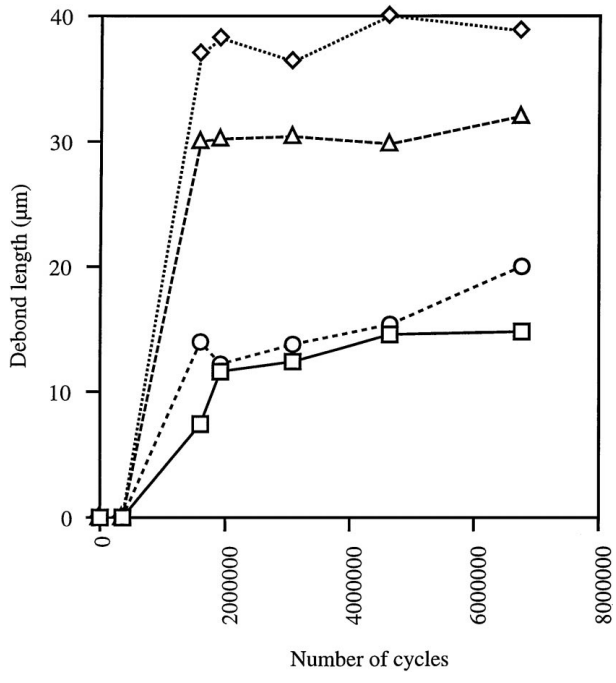

Figure 12 Debond propagation from a single fibre break in Region III in CF/epoxy ($\varepsilon = 0.89\%$).

scale, Curtis [12] identified the active fatigue damage mechanism in unidirectional CF/PEEK as longitudinal splitting, which started from defects. The results presented here explain this macroscopic damage mechanism by antecedent microscopic mechanisms, which are more closely related to the constituent properties and microstructure. This could give information of how to improve the fatigue behaviour by suppressing the progressive mechanisms through microstructural tailoring, e.g. improving the interfacial bond to restrain debond growth.

3.4. Comparison of fatigue behaviour and underlying mechanisms

Schematic illustrations of typical development of fatigue damage of the two composite systems are presented in Fig. 15. A feature which the two materials have in common is that the damage originates from fibre breaks. Since the fibres have a distribution in strength, some of them will break even at very moderate applied loads. If the applied strain level were low enough that no fibres would rupture, there would ideally be no ensuing damage, and the material would not fail in fatigue. However, the present study indicates that fibre breaks are always present.

The CF/epoxy shows a more brittle behaviour with small localized cracks originating from fibre breaks. These cracks propagate perpendicular to the fibre direction, and become bridged by the adjacent fibres. Conversely, the CF/PEEK has a tougher behaviour in the sense that it provides higher resistance to matrix crack growth. The damage accumulates instead on a larger scale as distributed multiple longitudinal cracks, with considerably more fibre breaks. The CF/PEEK shows a propensity to shear induced matrix cracking or debonding in the fibre direction. This is due to a lower matrix shear yield stress or a weaker interface compared to CF/epoxy [23]. The growth of longitudinal cracks will result in a continuous stress redistribution

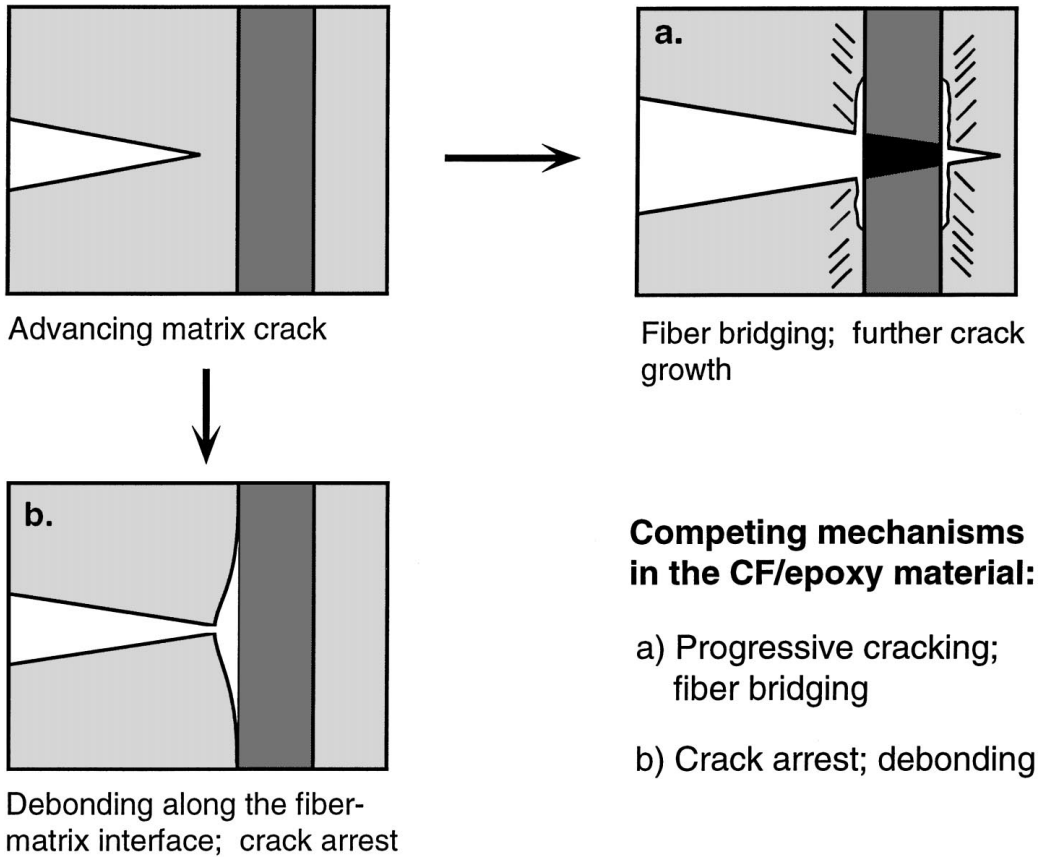

Figure 13 Alternative mechanisms as a matrix crack advances towards a fibre.

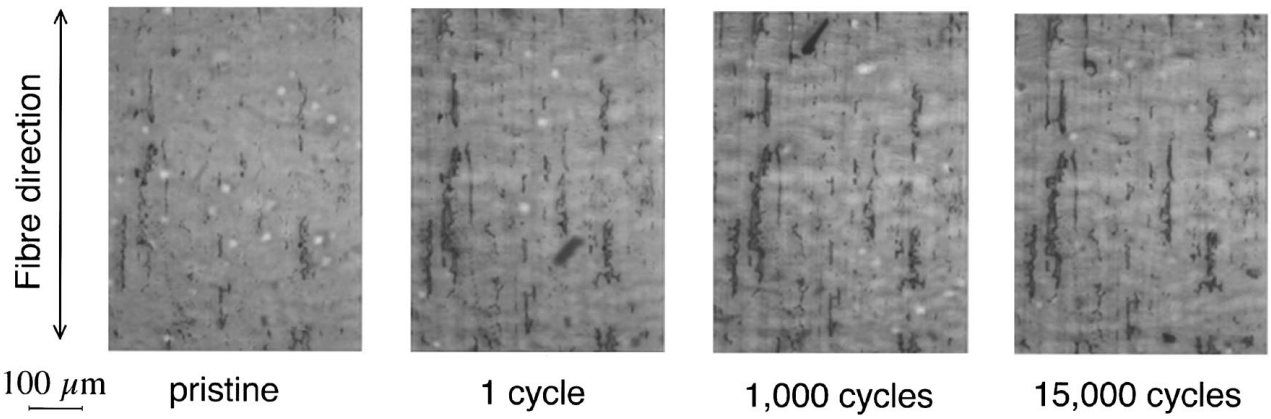

Figure 14 Debond or longitudinal matrix cracking in Region II in CF/PEEK ($\varepsilon = 0.96\%$).

in the neighbouring fibres, which may in turn fail and act as initiation points for further longitudinal crack growth. This progressive damage accumulation leads to a more pronounced sloping region in the fatigue life diagram. On the contrary, CF/epoxy has few damage sites on a small scale, and has therefore a more brittle behaviour. A perfectly brittle material either fails or is undamaged upon loading. Such a material has a flat horizontal scatter band in the fatigue life diagram. These trends with brittleness and the ability to progressively accumulate damage are manifested in the fatigue life data of CF/epoxy and CF/PEEK, respectively, in Fig. 2. The same trends have been observed in unidirectional glass-fibre reinforced plastics [24]. These observations support the contention that a composite material with a higher propensity to debond or longitudinal matrix crack growth become more fatigue sensitive. This qualitative link between micromechanisms and fatigue-life behaviour should in the future be established quantitatively by mechanistic modelling. A long term goal would be microstructural tailoring of the constituent properties for optimal fatigue performance based on such a quantitative model.

4. Conclusions

Microscopic and macroscopic fatigue investigations have been undertaken for unidirectional CF/epoxy and

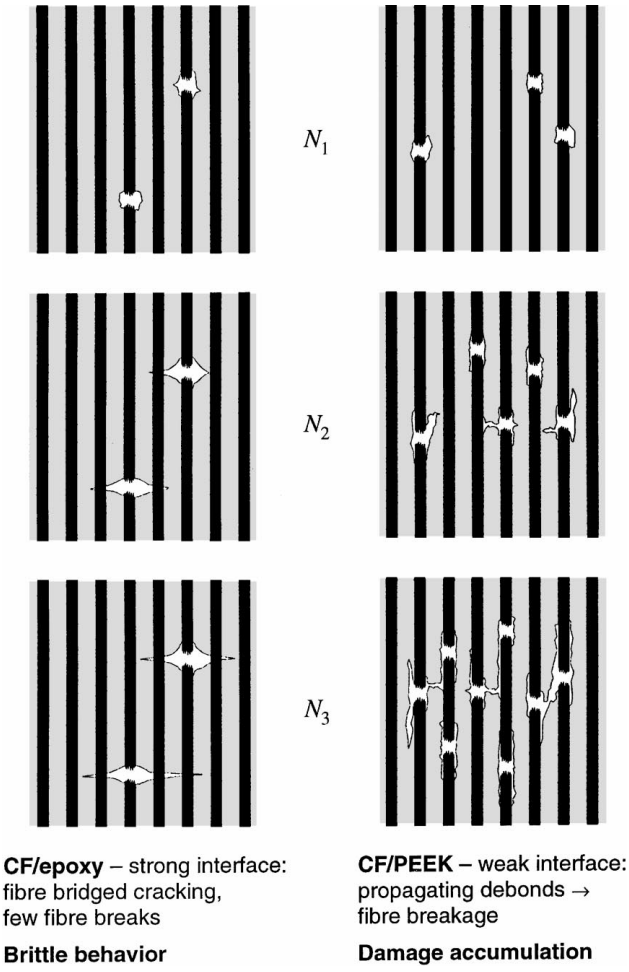

Figure 15 Schematic pictures of typical evolution of fatigue damage with increasing number of load cycles ($N_1 < N_2 < N_3$).

CF/PEEK loaded in tension-tension along the fibre direction. The observed micromechanisms were related to measured fatigue-life behaviour.

The fatigue damage mechanisms in CF/epoxy and CF/PEEK show some important differences. Small localized fibre-bridged cracks propagated in CF/epoxy, while CF/PEEK showed more extensive and distributed damage with progressive fibre breakage induced by longitudinal debonding or matrix cracking. Due to the relative progressiveness of damage and brittleness of the two materials, CF/PEEK has a steeper slope in the fatigue life diagram than that of CF/epoxy. Based on these and previous observations, it is suggested to choose composite constituents that suppress progressive debonding and longitudinal matrix cracking for better fatigue resistance.

Acknowledgements

Professor L. A. Berglund has contributed with valuable discussions and useful comment. Mr. Norbert Cabrera is gratefully acknowledged for help with manufacture and testing of the CF/PEEK material. One of the authors, E. K. Gamstedt, has received financial support from the Swedish Research Council for Engineering Sciences (TFR).

References

1. R. H. DAUSKARDT, R. O. RITCHIE and B. N. COX, *Adv. Mater. Process.* **7** (1993) 26.
2. R. TALREJA, *Proc. Roy. Soc. London* **A378** (1981) 461.
3. *Idem*., in "Structure and Properties of Composites," edited by T. W. Chou (VCH, Weinheim, 1993) p. 583.
4. R. F. DICKSON, G. FERNANDO, T. ADAM, H. REITER and B. HARRIS, *J. Mater. Sci.* **24** (1989) 227.
5. S. I. ANDERSEN, H. LILHOLT and A. LYSTRUP, in "Design of Composite Structures Against Fatigue," edited by R. M. Meyer (Mechanical Engineering Publications, Bury St. Edmunds, 1996) p. 15.
6. E. K. GAMSTEDT, PhD thesis No. 1997:36, Luleå University of Technology, 1998.
7. C. BARON, K. SCHULTE and H. HARIG, *Compos. Sci. Technol.* **29** (1987) 257.
8. A. J. RUSSEL and K. N. STREET, in "Toughened Composites," STP 937, edited by N. J. Johnston (ASTM, Philadelphia, 1987) p. 275.
9. M. HOJO, S. OCHIAI, C.-G. GUSTAFSON and K. TANAKA, *Eng. Fract. Mech.* **49** (1994) 35.
10. P. T. CURTIS, in Proceedings of the 6th International Conference on Composite Materials and 2nd European Conference on Composite Materials, London, July 1987, Vol. 4, p. 4.54.
11. B. HARRIS, H. REITER, T. ADAM, R. F. DICKSON and G. FERNANDO, *Composites* **21** (1990) 232.
12. P. T. CURTIS, *Int. J. Fatigue* **13** (1991) 377.
13. R. TALREJA, *Mater. Sci. Eng.* **A200** (1995) 21.
14. D. R. MOORE, in "Advanced Thermoplastic Composites: Characterization and Processing," edited by H. H. Kausch (Carl Hanser, Munich, 1993) p. 194.
15. A. TREGUB, H. HAREL, C. MIGLIARESI and G. MAROM, in Proceedings of the 9th International Conference on Composite Materials, Madrid, July 1993, edited by A. Miravete (Woodhead, Abington, 1993) Vol. 5, p. 677.
16. D. S. FARQUHAR, F. M. MUTRELLE, S. L. PHOENIX and R. L. SMITH, *J. Mater. Sci.* **24** (1989) 2151.
17. D. L. DAVIDSON, *Metall. Trans.* **23A** (1992) 865.
18. D. ZHENG and H. GHONEM, *Metall. Mater. Trans.* **26A** (1995) 2469.
19. B. N. COX and C. S. LO, *Acta Metall. Mater*. **40** (1992) 1487.
20. B. N. COX and D. B. MARSHALL, *Fatigue Fract. Eng. Mater. Struct.* **14** (1991) 847.
21. R. Y. KIM and J. T. HARTNESS, in Proceedings of the 29th National SAMPE Symposium and Exhibition, Reno, April 1984, p. 765.
22. L. LORENZO and H. T. HAHN, in "Composite Materials: Fatigue and Fracture," STP 907, edited by H. T. Hahn (ASTM, Philadelphia, 1986) p. 210.
23. P. VAUTEY and J. P. FAVRE, *Comp. Sci. Technol*. **38** (1990) 271.
24. E. K. GAMSTEDT, L. A. BERGLUND and T. PEIJS, in "Progress and Durability Analysis of Composite Systems," edited by K. L. Reifsnider, D. A. Dillard and A. H. Cardon (A. A. Balkema, Rotterdam, 1998) p. 137.

Received 18 August
and accepted 23 December 1998